Numerical Simulations of Wave Turbulence in Vibrating Plates

M. Ducceschi[1], C. Touzé[1], O. Cadot[1] & S. Bilbao[2]

[1] Unité de Mecanique, ENSTA - ParisTech, 828 Boulevard des Maréchaux, Palaiseau, France
[2] James Clerk Maxwell Building, University of Edinburgh, Scotland
michele.ducceschi@ensta-paristech.fr

Résumé. La turbulence d'ondes dans les vibrations de plaques minces est étudiée numériquement. Dans cette contribution, une méthode par différences finies est utilisée pour simuler les vibrations de plaques en grande amplitude, ce qui permet d'être plus proche de la réalité expérimentale comparativement aux résultats numériques déjà publiés. Des conditions aux limites de type simplement supporté sont imposées, et le forçage est ponctuel et harmonique. Un schéma temporel conservatif est utilisé, assurant une conservation parfaite de l'énergie discrète. Des simulations sans amortissement sont d'abord considérées afin de comparer aux résultats théoriques. L'absence d'amortissement permet d'engendrer une cascade d'énergie jusqu'à la fréquence de coupure numérique (proche de la fréquence de Nyquist). L'influence de paramètres géométriques comme l'épaisseur sur la puissance injectée et les spectres d'amplitude, est quantifiée. Des relations en terme de lois de puissance sont établies entre ces différentes grandeurs.

Abstract. This work is concerned with numerical simulations of wave turbulence in elastic plates. A finite difference code is used to simulate the turbulent regime of a plate vibrating at large amplitudes, hence allowing a computational framework that is closer to the experiments as compared to already published results. Physical boundary conditions are enforced, and the harmonic forcing is pointwise. An energy-conserving time-stepping scheme is used hence allowing for a perfect discrete conservation of energy in the conservative case. Undamped simulations are run first to check the numerical results with theoretical predictions. The absence of damping allows to generate an energy cascade up the numerical cutoff frequency (close to the Nyquist frequency). The influence of different geometrical parameters (*e.g.* the thickness) on derived quantities such, for instance, the injected power and the spectral amplitudes is quantified. Relations between these quantities is derived in the form of power laws.

1 Introduction

Wave Turbulence (WT) is a statistical description of the interactions amongst weakly nonlinear dispersive waves [1, 2]. This type of turbulence is in some aspects similar to the classical hydrodynamic turbulence, in that it describes a far-from-equilibrium set of random waves. The most salient feature of the WT description is that it is possible to find analytic solutions to the kinetic equations, from which a closed form for the power spectra corresponding to the energy cascade through lengthscales can be derived. Closure is generally not available in the broader context of hydrodynamic turbulence, where only dimensional arguments can be used to deduce the form of the spectra. Examples of WT systems range from water surface and capillary waves, Rossby waves, Alfvén waves, waves in nonlinear optics. Waves in nonlinear elastic plates also exhibit WT [6]: velocity power spectra have been analytically derived for infinite plates without dissipation. Early experiments on vibrating plates have shown however that the shape of the spectra differs significantly from the theory [4, 5]. The discrepancy has been attributed mainly to three contributions: finite-size effects, incorrect separation of the linear and nonlinear time scales, damping effects. This work presents early results derived from an energy-conserving finite difference scheme. The goal is to create a numerical setup that is as close as possible to a real experiment,

and where the plate parameters (viscous damping, geometry, imperfections ...) can be changed at will. This is a scheme that allows to simulate a framework that is much closer to the real experiments than earlier simulations presented in [6], relying on a pseudo-spectral scheme with periodic boundary conditions. Here physical boundary conditions are enforced, and the forcing is pointwise and harmonic as in the experiments.

In order to first verify the theoretical predictions, the code is run in the absence of damping. Energy is input at a grid point thanks to a sinusoidal forcing of ramping amplitude and whose frequency is tuned so to activate modal resonances in order to create more efficiently a turbulent state. The energy cascade is quantified in terms of cutoff frequencies calculated from the spectra. Self-similarity amongst spectra from different runs is checked. The injected power is calculated and used as descriptive parameter of the cascade, and its relation to the spectral amplitude (*e.g.* the amplitude at cutoff) is exploited.

2 Model Equations, WT Spectra and Numerical Setup

A plate whose flexural vibrations $w(\mathbf{x},t)$ are comparable to the thickness can be described efficiently by the von Kármán equations [7]. These are

$$D\Delta\Delta w(\mathbf{x},t) + \rho h\ddot{w}(\mathbf{x},t) = L(w,F) + P_{ext}(\mathbf{x},t); \tag{1a}$$

$$D\Delta\Delta F(\mathbf{x},t) = -\frac{Eh}{2}L(w,w), \tag{1b}$$

where $D = \sqrt{\frac{Eh^3}{12(1-\nu^2)}}$ is the plate rigidity, ρ is the material density, h is the thickness, E is Young's modulus, ν is the Poisson's ratio. F is the Airy stress function which quantifies the amount of motion in the in-plane direction. It is assumed that the thickness is much smaller than the plate dimensions ($h \ll L_x, L_y$). $L(\,\cdot\,,\,\cdot\,)$ is the von Kármán operator and reads

$$L(w,F) = w_{,xx}F_{,yy} + w_{,yy}F_{,xx} - 2w_{,xy}F_{,xy}, \tag{2}$$

where $_{,x} \equiv \frac{\partial}{\partial x}$. Note that the system so defined is undamped, but it presents an external forcing P_{ext} that is here realised as a pointwise sinusoid with ramping amplitude (see Fig. 1). Physical boundary

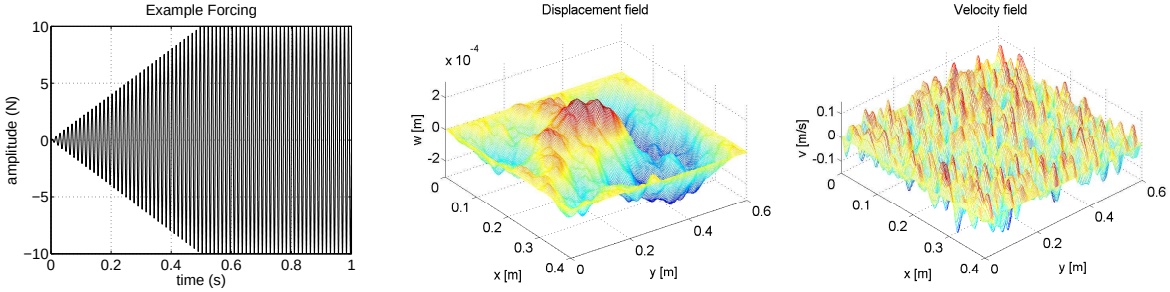

Figure 1. Forcing Amplitude for case 1 (left); typical displacement field (centre); typical velocity field (right).

conditions are chosen: they describe simply supported edges allowed to move in the in-plane direction.

Such a system is dispersive with linear dispersion relation given by:

$$\omega_{\mathbf{k}} = hc|\mathbf{k}|^2, \qquad c = \sqrt{\frac{E}{12(1-\nu^2)\rho}}. \tag{3}$$

The WT formalism allows to derive a form for the velocity power spectral density (PSD) spectra, $S_{vv}(f)$:

$$S_{vv}(f) \propto \epsilon^{1/3} \log^{1/3}\left(\frac{f_c}{f}\right), \tag{4}$$

where ϵ is the injected power, and f_c denotes some cutoff frequency *e.g.* the frequency of dissipation.

2.1 The Finite Difference Scheme

Time and space are discretised so that the continuous variables (x, y, t) are approximated by their discrete counterparts (lh_x, mh_y, nh_t), where (l, m, n) are integer indices and (h_x, h_y, h_t) are the steps. Boundedness of the domain implies that $(l, m) \in [0, N_x] \times [0, N_y]$ so that the grid size is given by $(N_x + 1) \times (N_y + 1)$. The continuous variables $w(\mathbf{x}, t)$, $F(\mathbf{x}, t)$ are then approximated by $w^n_{l,m}$, $F^n_{l,m}$ at the discrete time n for the grid point (l, m). Time shifting operators are introduces as

$$e_{t+} w^n_{l,m} = w^{n+1}_{l,m}, \qquad e_{t-} w^n_{l,m} = w^{n-1}_{l,m}. \tag{5}$$

Time derivatives can then by approximated by:

$$\delta_{t\cdot} = \frac{1}{2h_t}(e_{t+} - e_{t-}), \quad \delta_{t+} = \frac{1}{h_t}(e_{t+} - 1), \quad \delta_{t-} = \frac{1}{h_t}(1 - e_{t+}), \quad \delta_{tt} = \delta_{t+}\delta_{t-}. \tag{6}$$

Time averaging operators are introduced as:

$$\mu_{t+} = \frac{1}{2}(e_{t+} + 1), \quad \mu_{t-} = \frac{1}{2}(1 + e_{t-}), \quad \mu_{t\cdot} = \frac{1}{2}(e_{t+} + e_{t-}), \quad \mu_{tt} = \mu_{t+}\mu_{t-}. \tag{7}$$

Similar definitions hold for the space operators. Hence, the Laplacian Δ and the double Laplacian $\Delta\Delta$ are given by:

$$\delta_\Delta = \delta_{xx} + \delta_{yy}, \quad \delta_{\Delta\Delta} = \delta_\Delta \delta_\Delta. \tag{8}$$

The von Kármán operator at interior points $L(w, F)$ can then be discretised as:

$$l(w, F) = \delta_{xx} w \delta_{yy} F + \delta_{yy} w \delta_{xx} F - 2\mu_{x-}\mu_{y-}(\delta_{x+y+} w \delta_{x+y+} F). \tag{9}$$

Thus the discrete counterpart of eqs. (1) is:

$$D\delta_{\Delta\Delta} w + \rho h \delta_{tt} w = l(w, F) + F^n_{l,m}; \tag{10a}$$

$$\mu_{t-} D \delta_{\Delta\Delta} F = -\frac{Eh}{2} l(w, e_{t-} w). \tag{10b}$$

Such a scheme is stable and energy conserving, as proved in [3]. Implementation of boundary conditions is explained thoroughly in [3]. The first numerical experiments with the scheme have been used to investigate the transition to turbulence in plates [8].

2.2 Simulation Parameters

For this work, eight case studies are considered. Some plate parameters are kept constant in all simulations, and they are: density $\rho = 7860$ kg/m^3, Young's modulus $E = 2 \cdot 10^{11}$ Pa, Poisson's ratio $\nu = 0.3$, dimensions $L_x \times L_y = 0.4$ m $\times$ 0.6 m. The varying parameters are the maximum amplitude of forcing, the thickness, the injection frequency and the grid points. These are listed in Table 1. Note that the injection frequency changes with the thickness to always be around the 4^{th} eigenfrequency. Fig. 1 represents the first second of forcing for case 1, as well as typical displacement and velocity fields produced after the turbulent regime sets in. Note that the displacement field presents some traces of the eigenmodes of the plate, whereas the velocity field is much more homogeneous.

	Max Force (N)	Thickness (mm)	Excit. Freq (Hz)	Grid Points
Case 1	10	1	75	102×153
Case 2	20	1	75	102×153
Case 3	30	1	75	102×153
Case 4	45	1	75	102×153
Case 5	2.5	0.5	37.5	102×153
Case 6	5	0.5	37.5	102×153
Case 7	0.005	0.1	7.5	102×153
Case 8	0.02	0.1	7.5	144×215

Table 1. Case Studies

3 Simulation Analysis: Spectra, Energy Cascade, Injected Power

The first quantity used in the analysis is the *cutoff frequency* f_c. This is defined as:

$$f_c = \frac{\int_0^\infty f S_{vv}\, df}{\int_0^\infty f\, df}. \tag{11}$$

In this equation S_{vv} is (the estimate of) the PSD of the velocity v, whose theoretical behaviour is described by Eq. (4). The velocity is taken from one arbitrary point on the surface of the plate (not at the injection point). The cutoff frequencies so defined are time dependent as dissipation is absent. Fig. 2 pictures the cascade velocity in the turbulent state. It is found that the dependence is linear with time, as seen in Table 2.

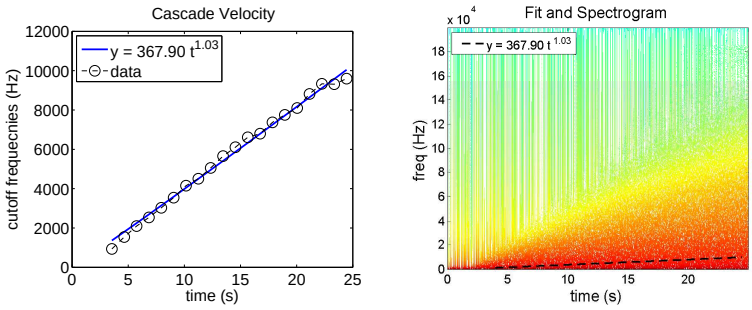

Figure 2. Cascade Velocity for case 1.

PSDs corresponding to case 1 are pictured in Fig. 3(a). The spectra tend to cover larger portions of the graph as time goes by: this happens because there is no dissipation and the energy keeps flowing to smaller wavelengths. Fig. 3(b) shows self similarity of the spectra when they are plotted on a normalised scale f/f_c and when the spectra are divided by their value at cutoff. The log correction and a power law with slope -0.2 are also plotted. Note that the slope from experimental data was found to be much larger, close to -0.5 [4]; so one could conclude that the presence of damping does affect the shape of the spectra. From the present analysis, the slope of the spectra is -0.2, a value which is consistent with the shape of the log correction. The spectral amplitude at cutoff was found to be a constant for each one of the case studies, with values reported in Table 2. The injected power is also considered. Table 2 reports the mean values and power law coefficients for the standard deviation. The standard deviation grows as $t^{0.4}$, as seen in Fig. 4(a) and (b) for case 1. When the mean injected power is plotted against the spectral amplitude, Fig. 4(c) is produced. A power law fit allows to conclude that

$$SA \propto \epsilon^{0.5}. \tag{12}$$

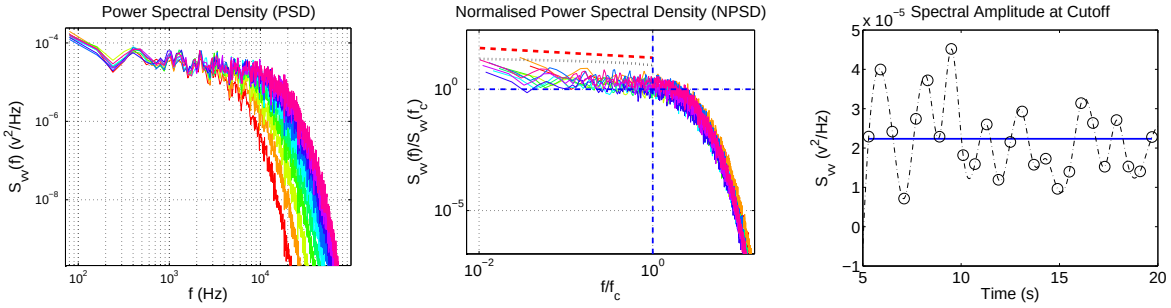

Figure 3. PSD for case 1 (left): note that the cutoff moves to higher frequencies as more modes are activated; NPSD for case 1 (centre) presenting the log correction (black dotted line) and a power law fit with slope -0.2 (red dashed line); spectral amplitude at cutoff for case 1 (right).

	$f_c = a\ t^b$		SA(f_c)	$<\epsilon>$ and $\epsilon_{rms} = c\ t^d$		
	a	b		Mean	c	d
Case 1	367.9	1.03	$2.02 \cdot 10^{-5}$	0.250	2.8	0.44
Case 2	778.9	0.92	$2.66 \cdot 10^{-5}$	0.393	7.9	0.42
Case 3	994.8	0.91	$2.78 \cdot 10^{-5}$	0.417	15	0.38
Case 4	1114.4	1.01	$3.39 \cdot 10^{-5}$	0.522	26	0.43
Case 5	320.0	0.91	$3.51 \cdot 10^{-6}$	$4.95 \cdot 10^{-3}$	0.28	0.37
Case 6	637.3	0.9	$6.53 \cdot 10^{-6}$	$6.32 \cdot 10^{-3}$	0.85	0.40
Case 7	18.19	0.92	$3.11 \cdot 10^{-8}$	$5.48 \cdot 10^{-7}$	$1.2 \cdot 10^{-5}$	0.42
Case 8	76.91	1.04	$1.08 \cdot 10^{-7}$	$3.61 \cdot 10^{-5}$	$2.6 \cdot 10^{-4}$	0.34
		avg: 0.95				avg: 0.40

Table 2. Results from fits: cutoff frequencies f_c grow linearly with time (left); values of the spectral amplitudes at cutoff (centre); mean values and standard deviation of the injected power ϵ (right).

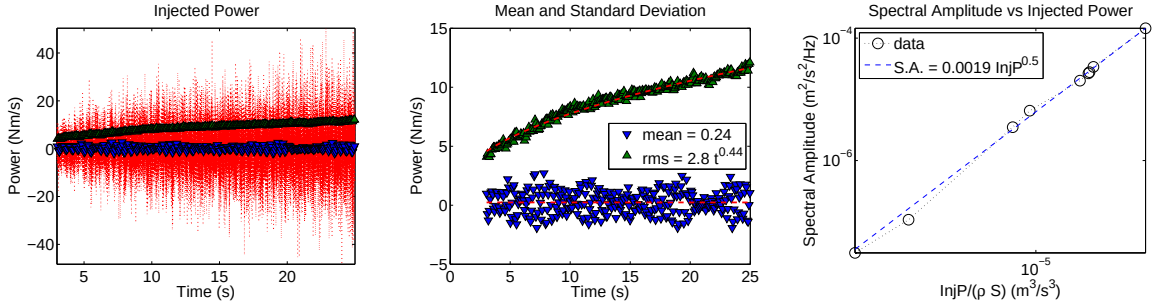

Figure 4. Injected Power for case 1 (left and centre); spectral amplitude as a function of the injected power (right).

4 Discussion and conclusion

Early-stage simulations of a turbulent elastic plate were presented. The plate was simulated thanks to a finite difference, energy conserving scheme with physical boundary conditions and pointwise forcing. Undamped simulations were run first to get rid of damping effects in the power spectra. Velocity Power Spectra were considered, and self-similarity was obtained after normalisation by the cutoff frequency (characteristic frequency of the end of the cascade). The slope of the spectra was found to be about -0.2, a value which resembles the log correction [6] and larger than the experimental value of -0.5 [4,5]. It is concluded that the damping has a large, yet undetermined effect on the slope of the experimental spectra. An important finding of the present simulation is that the spectra amplitude scales as $\epsilon^{\frac{1}{2}}$ instead

of the predicted scaling of $\epsilon^{\frac{1}{3}}$ obtained from the WT formalism [2,6]. Scaling with $\epsilon^{\frac{1}{2}}$ was also obtained in experiments [4,5]. Future work will focus on a test for homogeneity and isotropy of the velocity field; the relation of the injected power and its standard deviation will be investigated in terms of local and global energy fluxes. Finally, damping will be introduced in the scheme, as well as geometrical imperfections.

References

1. V. E. Zakharov, V. S. Lvov & G. Falkovisch, Kolmogorov Spectra of Turbulence I: Wave Turbulence, Springer, Berlin Heidelberg (1992).
2. S. Nazarenko, Wave Turbulence, *Lectures Notes in Physics*, Springer, Berlin Heidelberg (2011).
3. S. Bilbao, A family of conservative finite difference schemes for the dynamical von Kármán plate equations, *Numerical Methods for Partial Differential equations*, **24**, 1 (2008).
4. A. Boudaoud, O. Cadot, B. Odille & C. Touzé, Observation of Wave Turbulence in Vibrating Plates, *Phys. Rev. Lett.*, **100**, 234504 (2008).
5. N. Mordant, Are There Waves in Elastic Wave Turbulence?, *Phys. Rev. Lett.*, **100**, 234505 (2008).
6. G. Düring, C. Josserand & S. Rica, Weak turbulence for a vibrating plate: can one hear a Kolmogorov spectrum?, *Phys. Rev. Lett.*, **97**, 025503 (2006).
7. T. von Kármán, Festigkeitsprobleme im Maschinenbau, *Encyklopadie der Mathematischen Wissenschaften*, **4**, 4 (1910).
8. C. Touzé, O. Cadot & S. Bilbao, Transition scenario to turbulence in thin vibrating plates, *J. Sound Vib.*, **331**, 412–433 (2012).